PERGAMON

International Journal of Heat and Mass Transfer 42 (1999) 2863–2868

International Journal of HEAT and MASS TRANSFER

Thermal non-equilibrium effect on stabilities of falling liquid films

B.X. Wang*, J.T. Zhang, X.F. Peng

Thermal Engineering Department, Tsinghua University, Beijing 100084, People's Republic of China

Received 27 June 1998; in final form 12 October 1998

Abstract

Following our previous discussion and suggestion, the relationship between flow mode evolution and the Rayleigh number was theoretically investigated. From the simplified governing equations, analysis was conducted by using the singular theory. The results show that flow patterns of falling liquid films vary with the changing Rayleigh number. This analysis accounts rationally for the evolving processes of falling liquid films along a heated vertical wall.

Key words: Flow stability; Flow pattern; Falling liquid film; Heated vertical wall

Nomenclature

g gravity acceleration
L wavelength
n Ra/Ra_c
q heat flux
Ra Rayleigh number, $Ra = g\beta\Delta T_0\delta^3/v\alpha$
Re Reynolds number, $Re = 4\Gamma/\mu$
t time
t^* dimensionless time, $t^* = \alpha t/\delta^2$
x, z coordinates
x^*, z^* dimensionless coordinates.

Greek symbols

α thermal diffusivity
β coefficient of volume expansion
Γ liquid mass flow rate per unit width
δ average film thickness
ΔT_0 average temperature difference between heated wall and free interface
θ temperature departure
θ^* dimensionless temperature departure
μ dynamic viscosity
v kinetic viscosity
σ $\sigma = \delta/L$
Ψ stream function
Ψ^* dimensionless stream function.

1. Introduction

Falling liquid films cause wide concern nowadays for their high heat transfer capability. Some researches [1–5] show that falling liquid films can dramatically enhance heat transfer and have complex flow modes. Unfortunately, it is still difficult to explain the physical mechanism of the processes.

The stabilities of falling liquid films were comprehensively investigated widely in past decades. According to the theory of stability the falling films are unstable at any Reynolds number [6]. For very large Reynolds numbers ($Re > 1000$), the waves on falling films are of shear-waves with wavelengths comparable to or shorter than average film thickness. The interfacial dynamics would be dominated by the internal turbulence [7, 8]. At a moderate Reynolds number $1 < Re < 1000$, long interfacial waves of gravity–capillary instabilities appear [9]. Wave patterns near the inception line vary with different Reynolds numbers. The two-dimensional regular wave regimes are usually observed at $Re \sim 5$–20 near the wave inception line. In other cases, the film waves are three-dimensional and irregular [10]. The characteristics of falling liquid films are mainly described by the Rey-

* Corresponding author.

0017–9310/99/$ - see front matter
PII: S0017–9310(98)00346–9

nolds number which scales the ratio between inertia force and viscous force.

However, experimental results showed that flow patterns of falling liquid films are considerably complex [11] and the recent experiments [5] reveal that thermal conditions of a vertical wall have significant effects on interfacial waves.

We found [12] that the thermal non-equilibrium within liquid films might have an important effect on falling liquid films and hence, proposed to take *Ra* as an important parameter. In the present paper, singular theory was used to analyze the flow pattern evolution of falling liquid films along a heated vertical flat wall. The aim is to exhibit the role of thermal non-equilibrium on the stabilities of falling liquid films.

2. Theoretical considerations

2.1. Mathematical model

The governing equations for falling liquid films, shown in Fig. 1, are [12]

$$\nabla^2\frac{\partial\Psi^*}{\partial t^*}+\frac{\partial(\Psi^*,\nabla^2\Psi^*)}{\partial(x^*,z^*)}-Pr\frac{\partial\theta^*}{\partial x^*}+Ra\,Pr-Pr\,\nabla^4\Psi^*=0 \tag{1}$$

$$\frac{\partial\theta^*}{\partial t^*}+\frac{\partial(\Psi^*,\theta^*)}{\partial(x^*,z^*)}+Ra\frac{\partial\Psi^*}{\partial z^*}-\nabla^2\theta^*=0 \tag{2}$$

where the dimensionless stream function is defined as $\Psi^*=\Psi/\alpha$, in which Ψ is a stream function and α is thermal diffusivity of liquid. θ^* is a dimensionless temperature, defined as $\theta^*=\theta/[\alpha\nu/g\beta\delta^3]$, in which θ is a temperature departure from the average value, δ is an average film thickness, β and ν are the coefficients of volume expansion and kinetic viscosity of liquid, respectively, g is the gravity acceleration, t^* is the dimensionless time scale, $t^*=t/[\delta^2/\alpha]$, $x^*=x/\delta$ and $z^*=z/\delta$ are dimensionless coordinates.

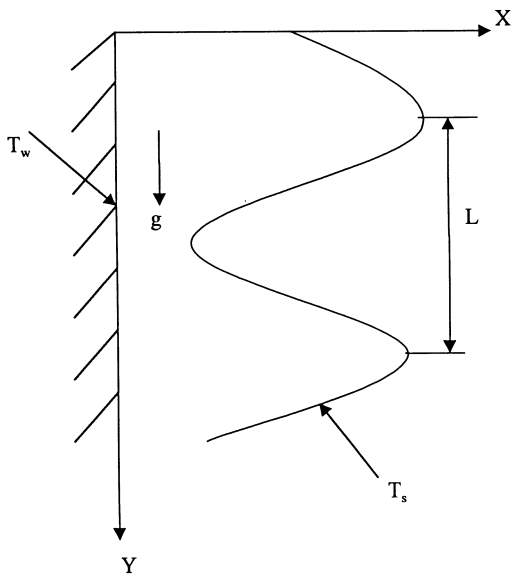

Fig. 1. Physical model for analysis.

Here, $Pr=\nu/\alpha$ and $Ra=g\beta\delta^3\Delta T_0/\alpha^2$ are considered as the independent parameters in the present model. Generally, *Pr* could be taken as a constant for a given liquid. Hence, *Ra* is the principal parameter to reveal the effect of thermal non-equilibrium on the evolution of falling films.

The above-mentioned analytical model is analogous to that of Saltzman [13]. Lorenz [14] reduced the analytical model of Saltzman [13] to a group of finite dimensional non-linear equations and solved numerically to explore the flow pattern evolution with *Ra*, varied from simple periodic flow to complex periodic flow and finally to chaotic flow. The method proposed by Lorenz [14] was employed to analyze falling liquid films in this paper.

2.2. Reduction of equation

In equation (1), the fourth term on the left, *Ra Pr*, would be a constant, for a given falling liquid film and can be eliminated by differentiating the equation with respect to x^*. As a result, equation (1) could be reduced to

$$\frac{\partial}{\partial x^*}\left(\nabla^2\frac{\partial\Psi^*}{\partial t^*}+\frac{\partial(\Psi^*,\nabla^2\Psi^*)}{\partial(x^*,z^*)}-Pr\frac{\partial\theta^*}{\partial x^*}-Pr\,\nabla^4\Psi^*\right)=0. \tag{3}$$

Referring to Saltzman [13], the stream function Ψ^* and temperature θ^* can be represented as a sum of double-Fourier components. For turbulence, small wave numbers and big scale vortices play the principal role in the formation and transfer of turbulent energy and Reynolds shear stress. It is reasonable to expect that big vortices play the main role in the evolution of falling liquid films. Therefore, Ψ^* and θ^* can be truncated under low dimension by referring to Lorenz's investigation [14]. We obtain

$$\frac{\sigma}{1+\sigma^*}\Psi^*=\sqrt{2}X(t^*)\sin(\pi x^*)\sin(\sigma\pi z^*) \tag{4}$$

$$\frac{\sigma}{(1+\sigma^2)^3\pi^3}\theta^*=\sqrt{2}Y(t^*)\cos(\pi x^*)\sin(\sigma\pi z^*)-Z(t^*)\sin(2\sigma\pi z^*) \tag{5}$$

where $\sigma=\delta/L$.

Substitute equations (4) and (5) into equations (3) and (2). Omitting the trigonometric terms other than those occurring in (4) and (5), we obtain

$$\frac{dX}{d\tau} = -Pr\,X + Pr\,Y$$

$$\frac{dY}{d\tau} = \mu X - Y - XZ$$

$$\frac{dZ}{d\tau} = -bZ + XY \tag{6}$$

where $\tau = \pi^2(1+\sigma^2)t^*$. $b = 4\sigma/(1+\sigma^2)$, $n = Ra/Ra_c$. $Ra_c = \pi^4(1+\sigma^2)^3/\sigma$.

3. Singular analysis

Water was chosen as a working fluid, with $Pr = 7.0$. As the wave thickness is comparable to the wavelength [9], the ratio of the average film thickness to the wavelength can reasonably be chosen as $\sigma = 0.707(\sigma^2 = 1/2$ [14]). This results in $Ra_c = 465$. Referring to Ott [15], equation (6) has three positive steady states. They are

$$\begin{aligned} O(X_0, Y_0, Z_0) &= (0,0,0) \\ P^+(X_{P^+}, Y_{P^+}, Z_{P^+}) &= (\sqrt{b(n-1)}, \sqrt{b(n-1)}, n-1) \\ &\quad (n > 1) \\ P^-(X_{P^-}, Y_{P^-}, Z_{P^-}) &= (-\sqrt{b(n-1)}, -\sqrt{b(n-1)}, n-1) \\ &\quad (n < 1). \end{aligned} \tag{7}$$

Pr and b will be constants for a given falling liquid film. So, the behavior of the system could be examined by changing the value of n. The stability of the steady state O is given by the eigenvalues of the Jacobian matrix

$$J_1 = \begin{bmatrix} -Pr & Pr & 0 \\ n & -1 & 0 \\ 0 & 0 & -b \end{bmatrix}.$$

The eigenvalue equation would be

$$(S+b)[S^2 + (Pr+1)S + Pr(1-\mu)] = 0. \tag{8}$$

The three roots of equation (8) are

$$\begin{aligned} S_1 &= -b \\ S_2 &= \tfrac{1}{2}[-(Pr+1) + \sqrt{(Pr+1)^2 - 4\,Pr(1-n)}] \\ S_3 &= \tfrac{1}{3}[-(Pr+1) - \sqrt{(Pr+1)^2 - 4\,Pr(1-n)}] \end{aligned} \tag{9}$$

S_1, S_2 and S_3 are all negative for $0 < n < 1$, which indicates the stead state O being the only attractor of the system. As n passes through 1, S_2 becomes positive with the other two remaining negative. This indicates that O has a two-dimensional stable manifold and a one-dimensional unstable manifold. Along with the loss of stability of O, the two fixed points P^+ and P^- are born. The Jacobian matrix of point P^+ and P^- is

$$J_2 = \begin{bmatrix} -Pr & Pr & 0 \\ 1 & -1 & \mp\sqrt{b(n-1)} \\ \pm\sqrt{b(n-1)} & \pm\sqrt{b(n-1)} & -b \end{bmatrix}$$

and accordingly, the equivalent eigenvalue equation would be

$$S^3 + (Pr+b+1)S^2 + b(Pr+n)S + 2b\,Pr(n-1). \tag{10}$$

Obviously, all coefficients of the eigenvalue equation are positive when $n > 1$. Equation (10) must have a negative root and the other two roots are negative if

$$\frac{p^3}{27} + \frac{q^2}{4} \leqslant 0$$

$$p = b(n+Pr) - \frac{1}{3}(Pr+b+1)^2$$

$$q = 2b\,Pr(n-1) - \frac{b}{3}(\mu+Pr)(Pr+b+1) + \frac{1}{27}(Pr+b+1)^3. \tag{11}$$

From equation (11), we have $n \leqslant n_1 = 1.255$. Hence, the states P^+ and P^- are stable under the condition $1 < n \leqslant 1.255$ and thereby become the attractors of the system. Following the unstable manifold of O, it goes to the steady state of P^+ and P^-. As n increases further, two negative eigenvalues of P^+ and P^- coalesce and become complex conjugate eigenvalues with negative real parts. In this regime, orbits approach P^+ and P^- by spiraling around them.

If n is slightly greater than n_1, equation (10) has a negative eigenvalue and a couple of complex conjugate eigenvalues

$$S_1 < 0, \quad S_2 = S_r + iS_i \quad \text{and} \quad S_3 = S_r - iS_i$$

where the real part, $S_r < 0$. Hence, P^+ and P^- become a stable focus. The eigenvalue equation can be written as

$$(S-S_0)(S-S_r-iS_i)(S-S_r+iS_i) = 0. \tag{12}$$

Rearranging, it yields

$$S^3 - (S_0+2S_r)S^2 + (2S_0S_r + S_i^2 + S_r^2)S - S_0(S_r^2+S_i^2) = 0. \tag{13}$$

Comparing the coefficients of equations (13) and (10), we have

$$\begin{aligned} Pr+b+1 &= -(S_1+2S_0) \\ b(n+Pr) &= 2S_1S_r + S_i^2 + S_r^2 \\ 2b\,Pr(n-1) &= -S_1(S_r^2+S_i^2). \end{aligned} \tag{14}$$

When $S_r = 0$, the following expressions were derived

$$n_2 = \frac{Pr(Pr+b+3)}{Pr-b-1} = 20.22$$

$$\left.\frac{\partial S_r}{\partial n}\right|_{n=n_2} = \frac{b(Pr-b-1)}{2[b(n_2+b)+(Pr+b+1)]^2} > 0. \tag{15}$$

That is, increasing n still further, the steady states P^+ and P^- become unstable at $n = n_2 = 20.22$ for the real parts of their complex conjugate eigenvalues pass from negative to positive (a Hopf bifurcation). P^+ and P^- become

unstable through stable. As n increases further through n_2, the system gets into a chaotic regime. There is only one chaotic attractor. The orbits around P^+ and P^- behave irregularly to form a local unstable but intact stable chaotic attractor.

4. Numerical integration

The behavior of the manifold of O, P^+ and P^- has been discussed analytically above, that is as n is greater than $n = 20.22$, the system becomes chaotic. As an example, to illustrate the chaotic orbits, a numerical integration procedure was employed to solve the non-linear equation (6) under the condition $n = 21$ for water. Using the Runge–Kutta procedure, the dimensionless time increment Δt^* is equal to 0.01. The initial conditions were chosen as a slight departure from the steady state of no attraction, namely $(0, 1, 0)$ and $(0, -1, 0)$. The number of iteration was chosen as 3000. The coordinate of the two steady states P^+ and P^- are $(6.1410, 6.1410, 20)$ and $(-6.1410, -6.1410, 20)$, respectively. The instability of the system is evident. Figure 2 shows the trajectory in phase space corresponding to iterations 1–3000. All three variables grow rapidly at first and then move around the attractor with irregular orbits. If the initial point is $(0, 1, 0)$, the point (X, Y, Z) quickly approaches the steady state P^- $(-6.1410, -6.1410, 20)$ and then moves around P^-. The motion of the point (X, Y, Z) is spiral and irregular. Evidently, the state P^- is the chaotic attractor under this condition. If the initial point is $(0, -1, 0)$, the point (X, Y, Z) similarly goes to the steady state P^+ $(6.1410, 6.1410, 20)$ soon and then moves around the steady state. Figures 4 and 5 show the projections of the trajectories on the x–y plane. The black area around attractor P^+ or P^- indicates the chaotic motion of the dynamic system. Obviously, the trajectory around P^+ is the same with that around P^-. They have the same physical significance.

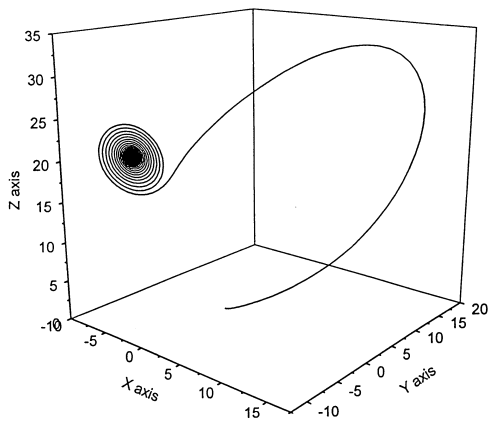

Fig. 2. Trajectory of initial point $(0, 1, 0)$.

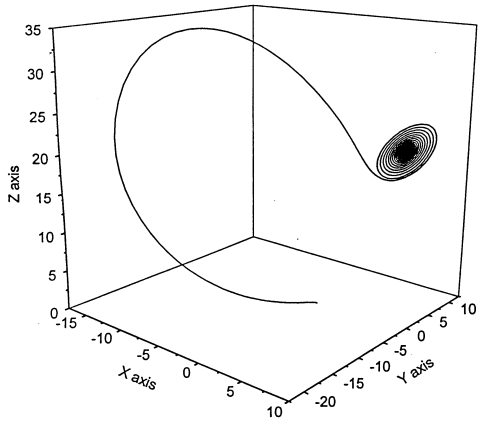

Fig. 3. Trajectory of initial point $(0, -1, 0)$.

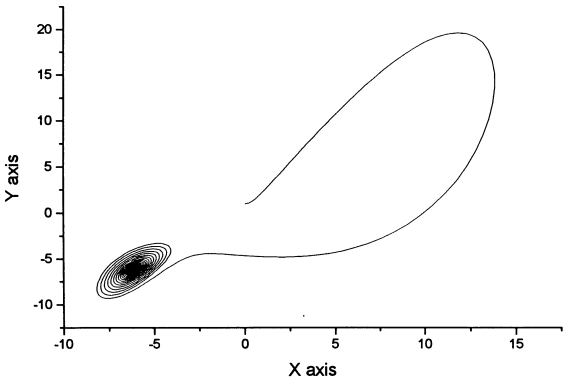

Fig. 4. Projection of the trajectory of $(0, 1, 0)$ on X–Y plane.

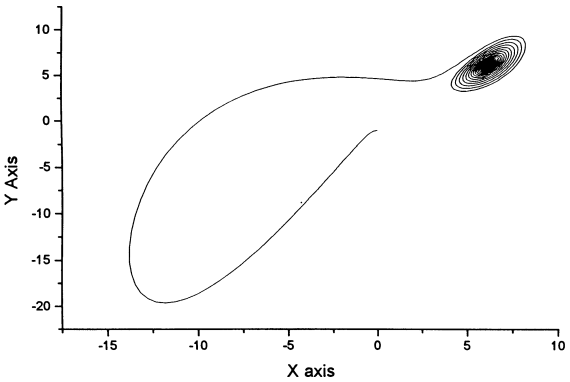

Fig. 5. Projection of the trajectory of $(0, -1, 0)$ on X–Y plane.

The procedure proposed by Badii and Politi [16] was adopted to calculate the fractal dimension of the chaotic

system. For a system described by three first-order ordinary differential equations, the attractor will be a line and hence, of one dimension when the motion is periodic and quasiperiodic motion made up of two non-harmonic frequencies will form a two-dimensional torus. If the process is one displaying deterministic chaos, the dimension of the attractor falls between two and three. On the other hand, if the process is statistically random, then the attractor will fill the entire phase space and its dimension will be three.

The phase space is constituted by (X, Y, Z). According to the nearest-neighbor method of Badii and Politi [16] a set of N points of the attractor was chosen and a point x on this attractor is arbitrarily selected as a reference point. Choose at random a subset of k points denoted by y_i ($i = 1, 2, \ldots, k$ and $k < N$) from the original set of N points and consider the distance from x to each point y_i. Define

$$D = \min \|x - y_i\| \tag{16}$$

D is the distance to the nearest neighbor. In order to obtain a statistically useful value of the minimum distance, calculation is repeated over many randomly chosen reference points to obtain the average D_a. The process is then repeated for a sequence of k values up to $k = N-1$ for each x. The number of nearest neighbors contained in m-dimensional hypersphere of radius D around a given point should vary as D^d if the attractor is d-dimensional. It is argued that

$$D_a \sim k^{(-1/d)} \tag{17}$$

and hence,

$$d = -\lim \frac{\log k}{\log D_a}. \tag{18}$$

The negative, inverse slope of a $\log D_a$ vs. $\log k$ plot is the fractal dimension.

The calculated fractal dimension of the system under the condition $n = 21$ is 2.39. This means that as n is greater than 20.22, the system gets into chaos. The result is consistent with that of the above mentioned singular analysis in Section 3.

5. Comparison with discussion

These projections are compared with that of the experimental results, obtained by Lacy and Dulker [2] from a measured film thickness time series. We realize that the calculated trajectory is analogous to that from the experiment.

The present results indicate that thermal non-equilibrium has an important effect on stabilities of falling liquid films, as we previously pointed out [12]. The experimental results of Lyu and Mudawar [5] show that liquid temperatures within films vary oppositely to the variation of film thickness. For a given Reynolds number, the temperature fluctuation increased monotonically as heat flux, q, was increased to steady-state values between 0 and 75 000 W m^{-2}. The effect of interfacial waves on liquid temperature was most significant for $Re \leqslant 5000$ and less noticeable for $Re \geqslant 10\,000$, even at heat fluxes in relatively high values of 50 000 W m^{-2}. Probability density distributions of film thickness are sensitive to heat fluxes at relatively low Re ($Re < 5000$), but rather invariant with heat fluxes for $Re \geqslant 5000$. Increasing heat flux also enhances the relationship between thickness and temperature. Lyu and Mudawar [5] commented on the role of heat flux to falling liquid films. One suggestion is that increasing the flux raises the liquid temperature, resulting in a lower kinetic viscosity and consequently, a higher Reynolds number. Another suggestion is that heating could also affect the hydrodynamic structure of the interfacial waves due to the change in kinetic viscosity and surface tension and so, the surface tension temperature gradients. The experimental results indicate that the Reynolds number is not the only dimensionless parameter influencing the flow and heat transfer for falling liquid films.

The present analysis shows that, as the Rayleigh number increases up to the critical point, $Ra_c = 465$ for water, the steady state of liquid film changes and converts to another steady state. The corresponding flow patterns convert from smooth form to wavy form. As the Ra increases further, the simple wavy flow becomes complex wavy flow. Eventually, as the Rayleigh number increases up to 9400, the flow evolves into chaos. The analyses clearly reveal that the Rayleigh number would be an important parameter in falling liquid films.

Noting, for simplification of the problem, the governing equations were severely truncated and the high wave number terms were neglected. It is not clear how much the severe truncation will affect the analytical results. Because of the effect of the high wave number terms, the periodic wavy flow might not exist and be replaced by quasiperiodic wavy flow. Further, the thermocapillarity and evaporation on the free interface were not taken into account. We know thermocapillarity is an important destabilizing factor. It makes wavy films more distorted and irregular. Hence, the value of the practical critical Rayleigh number might be different from that of the analytical result for the influence. Further experimental and theoretical works will be needed.

6. Conclusion

Conclusions reached can be summarized as:

(1) the thermal non-equilibrium should play an important role in falling liquid films;
(2) the Rayleigh number might be a principal dimen-

sionless parameter in falling liquid films along a heated vertical flat wall;
(3) flow patterns of falling liquid films vary with changes of the Rayleigh number;
(4) further experimental and theoretical investigations are urgently needed.

Acknowledgements

This project is financially supported by the Fundamental Research Fund from the Ministry of Education, China and also partly from Tsinghua University, Beijing.

References

[1] K.J. Chu, A.E. Dukler, Statistical characteristics of thin wavy films, Part I. Studies of the substrate and its wave structure, AIChE J. 20 (1974) 695–706.
[2] C.E. Lacy, M. Sheinsuch, A.E. Dukler, Methods of deterministic chaos applied to the flow of thin wavy films, AIChE J. 37 (4) (1991) 481–489.
[3] F.K. Wasden, A.E. Dukler, Insight into the hydrodynamics of free falling wavy films, AIChE J. 35 (2) (1989) 187–195.
[4] S. Jayanti, G.F. Hewitt, Hydrodynamics and heat transfer of wavy thin film flow, Int. J. Heat Mass Transfer 40 (1) (1997) 179–190.
[5] T.H. Lyu, I. Mudawar, Statistical investigation of the relationship between interfacial waviness and sensible heat transfer to a falling liquid film, Int. J. Heat Mass Transfer 34 (6) (1991) 1451–1464.
[6] P. Van Carey, Liquid–Vapor Phase-Change Phenomena: An Introduction to the Thermophysics of Vaporization and Condensation Processes in Heat Transfer Equipment, Hemisphere, 1992, pp. 112–120.
[7] J.R. Berschy, R.W. Chin, F.W. Abernathy, High-strain-rate free-surface boundary-layer flows, J. Fluid Mech. 126 (1983) 443–461.
[8] J.M. Floryan, S.H. Davis, R.E. Kelly, Instabilities of a liquid film flowing down a slightly inclined plane, Phys. Fluids 30 (4) (1987) 983–989.
[9] H.-C. Chang, Wave evolution on a falling film, Annu. Rev. Fluid Mech. 26 (1994) 103–136.
[10] S.V. Alekseenko, V.E. Nakoryakov, B.G. Pokusaev, Wave formation on falling liquid films, Int. J. Multiphase Flow 11(5) (1985) 607–627.
[11] H. Takahama, S. Kato, Longitudinal flow characteristics of falling liquid films without concurrent gas flow, Int. J. Multiphase Flow 6 (3) (1980) 203–215.
[12] B.X. Wang, J.T. Zhang, X.F. Peng, On the effect of lateral thermal convection on freely falling liquid film flow, Int. J. Heat Mass Transfer 41 (23) (1998) 4031–4033.
[13] B. Saltzman, Finite amplitude free convection as an initial value problem—I, J. Atmospheric Science 19 (7) (1961) 329–341.
[14] E.N. Lorenz, Deterministic nonperiodic flow, J. Atmospheric Science 20 (3) (1961) 131–141.
[15] E. Ott, Chaos in Dynamical Systems, Cambridge University Press, 1993, pp. 291–294.
[16] R. Badii, A. Politi, Statistical description of chaotic attractors: the dimension function, J. Statistical Physics 40 (5/6) (1985) 725–750.